NIH Public Access
Author Manuscript

Interleukin (IL)-1 and IL-6 regulation of neural progenitor cell proliferation with hippocampal injury: Differential regulatory pathways in the subgranular zone (SGZ) of the adolescent and mature mouse brain

CA McPherson[a,b], **M Aoyama**[a,c], and **GJ Harry**[a,*]

[a]Neurotoxicology Group, Laboratory of Toxicology and Pharmacology, National Institute of Environmental Health Sciences, National Institutes of Health

[b]Curriculum in Toxicology, University of North Carolina at Chapel Hill, Chapel Hill, NC

[c]Department of Molecular Neurobiology, Nagoya City University, Nagoya, Japan

Abstract

Current data suggests an association between elevations in interleukin 1 (IL-1)α, IL-1β, and IL-6 and the proliferation of neural progenitor cells (NPCs) following brain injury. A limited amount of work implicates changes in these pro-inflammatory responses with diminished NPC proliferation observed as a function of aging. In the current study, adolescent (21 day-old) and 1 yr-old CD1 male mice were injected with trimethyltin (TMT, 2.3 mg/kg, i.p.) to produce acute apoptosis of hippocampal dentate granule cells. In this model, fewer 5-bromo-2′-deoxyuridine (BrdU)$^+$ NPC were observed in both naive and injured adult hippocampus as compared to the corresponding number seen in adolescent mice. At 48 h post-TMT, a similar level of neuronal death was observed across ages, yet activated amoeboid microglia were observed in the adolescent and hypertrophic process-bearing microglia in the adult. IL-1α mRNA levels were elevated in the adolescent hippocampus; IL-6 mRNA levels were elevated in the adult. In subgranular zone (SGZ) isolated by laser-capture microdissection, IL-1β was detected but not elevated by TMT, IL-1α was elevated at both ages, while IL-6 was elevated only in the adult. Naïve NPCs isolated from the hippocampus expressed transcripts for IL-1R1, IL-6Rα, and gp-130 with significantly higher levels of IL-6Rα mRNA in the adult. *In vitro*, IL-1α (150pg/ml) stimulated proliferation of adolescent NPCs; IL-6 (10ng/ml) inhibited proliferation of adolescent and adult NPCs. Microarray analysis of SGZ post-TMT indicated a prominence of IL-1α/IL-1R1 signaling in the adolescent and IL-6/gp130 signaling in the adult.

Keywords

neurogenesis; neurospheres; hippocampus; apoptosis; neuroinflammation; SGZ; interleukin-1; interleukin 6; gp130

*Corresponding address: National Institute of Environmental Health Sciences, P.O. Box 12233, MD C1-04, Research Triangle Park, NC 27709. Ph. (919) 541-0927, Fax. (919) 541-4634, harry@niehs.nih.gov. .

1. Introduction

Adult hippocampal neurogenesis is initiated with the proliferation of neural progenitor cells (NPCs) within the subgranular zone (SGZ) of the dentate gyrus leading to the formation of new dentate granule neurons. Regulation of this process in the normal control brain and following injury occurs via numerous secreted factors such as hormones (Cameron and Gould, 1994), neurotransmitters (Banasr et al., 2004; Yoshimizu and Chaki, 2004), growth factors (Aberg et al., 2000; Larsson et al., 2002), and cytokines (Das and Basu, 2008; Kaneko et al., 2006; Mathieu et al., 2010; Taupin, 2008). Though not fully understood at this time, regulation of this process through either cellular components such as microglia and astrocytes (Alvarez-Buylla and Lim, 2004) or secreted factors is known to be critical for hippocampal neurogenesis following brain injury, and is thought to contribute to the capacity for "self-repair" of the dentate granule neurons (Ming and Song, 2005).

Associated with the regulation of NPCs in the hippocampus following injury is often the concurrent activation of microglia. Microglia serve as the resident immune cells of the brain and upon injury they shift to a reactive phenotype (Davalos et al., 2005; Nimmerjahn et al., 2005). Upon activation these cells produce pro-inflammatory cytokines including interleukin-1β (IL-1β), interleukin-1α (IL-1α), and interleukin-6 (IL-6) (Mrak and Griffin, 2005). Overall, the literature indicates IL-1β, IL-1α, and IL-6 adversely affects neurogenesis by altering proliferation, survival, differentiation, and functional aspects of NPCs (Ajmone-Cat et al., 2010; Das and Basu, 2008; Mathieu et al., 2010). Recent studies examining the specificity of these effects on NPC proliferation support the critical modulatory effects of neuroinflammation (Monje et al., 2003) and targeted effects of IL-1 and IL-6 signaling (Monje et al., 2003; Spulber et al., 2008). Upon activation of microglia by lipopolysaccharride (LPS) to release pro-inflammatory cytokines, a direct inhibition of NPC proliferation has been observed (Cacci et al., 2005; Monje et al., 2003). In addition, this inhibition is associated with an enhanced differentiation of NPC to the glial lineage. A similar decline in NPC proliferation has been demonstrated in the hippocampus *in vivo* in transgenic mice over-expressing IL-6 in astrocytes (Vallieres et al., 2002). Further examination of the modulation effects of IL-1β showed that the inhibition of NPC proliferation is the result of downstream signaling events occurring following the activation of IL-1 receptor 1 (IL-1R1) (Koo and Duman, 2008). These effects of IL-1R1 activation have not necessarily been translated *in vivo* in that transgenic mice over-expressing IL-1 receptor antagonist (IL-1Ra) demonstrated diminished NPC proliferation following an excitotoxic injury (Spulber et al., 2008). The work of Spulber et al (2008) was the first to suggest that the effect of IL-1R1 signaling on NPCs was conditional on the age of the animal. Under non-injury conditions, the basal level of hippocampal NPC proliferation was significantly diminished in 5 month-old IL-1Ra transgenic mice and by 22 months-of-age, this difference was no longer evident.

Studies have demonstrated diminished hippocampal NPC proliferation as a function of aging from the adolescent/young adult to the adult rodent (Hattiangady et al., 2008; He and Crews, 2007; Kuhn et al., 1996) and brain insult (Hattiangady et al., 2008; Shetty et al., 2010). These studies clearly demonstrate an ontogeny in the level of hippocampal NPC proliferation that has only been marginally examined within the framework of a coordinated development of the proliferative SGZ, the dentate granule cell layer, and microglia. The proliferative zone of the hippocampus is established between the 2nd and 4th week following birth when precursor cells of dentate granule neurons populate the SGZ of the rodent (Schlessinger et al., 1975). The dentate granule cell layer (GCL) is also established during this same age period. Concurrent with these developmental processes, microglia are proliferating rapidly and establishing a unique nervous system identity primarily between postnatal days 5 to 20 (Lawson et al., 1990). The impact of these coordinated development

events on the response of hippocampal NPC to injury and the associated elevation of pro-inflammatory cytokines due to maturing microglia has not been adequately examined.

To address these questions, we compared changes in the SGZ in the adolescent (21 day-old) and the adult (1 yr-old) CD-1 male mouse following a localized damage to the dentate granule neurons. We utilized the hippocampal toxicant, trimethyltin (TMT) to produce hippocampal damage, elevate pro-inflammatory cytokines, and induce the proliferation of NPC within the SGZ (Harry and Lefebvre d'Hellencourt, 2003; Harry et al., 2004; McPherson et al., 2010). Using this injury model, an elevation of IL-1α signaling via IL-1R1 and downstream genes within the IκB/NFkB1 signaling pathway were observed in the SGZ of 21 day-old mice. An alternative pathway was activated in 1 yr-old mice, with an upregulation of IL-6/gp130 signaling via the Ras/MAPK pathway. When we compared the effects of IL-1α and IL-6 on the *in vitro* proliferation of NPCs obtained from the hippocampus of adolescent and adult mice, a induction of NPC proliferation was observed with IL-1α and a specific inhibition of NPC proliferation was seen in the 1 yr-old mice. Thus, our data demonstrates an age-related shift in IL-1α and IL-6 signaling within the SGZ supporting a differential effect of pro-inflammatory cytokines on hippocampal NPC self-renewal following injury.

2. Materials and Methods

2.1. Animals

Male adolescent (21 day-old) and adult (1 yr-old) CD-1 mice were obtained from Charles River Laboratories (Raleigh, NC). Mice were individually housed in a dual corridor, semi-barrier animal facility with food (autoclaved NIH 31 rodent chow) and deionized, reverse osmotic-treated water available *ad libitum*. Sentinel animals recorded negative for pathogenic bacteria, mycoplasma, viruses, ectoparasites, and endoparasites. All procedures were conducted in compliance with NIEHS/NIH Animal Care and Use Committee approved animal protocol.

2.2. Model of dentate granule cell death

Mice received a single intraperitoneal (i.p.) injection of either 2.3 mg/kg trimethyltin hydroxide (TMT; Alfa Products, Danvers, MA) or vehicle (saline), in a dosing volume of 2 ml/kg body weight using a 50 μL Hamilton syringe. Tremor was evident at 24 h post-TMT with no acute morbidity. All endpoints were examined at 48 h post-dosing time point.

2.3. Tissue fixation and sectioning

Mice were anesthetized with CO_2 and decapitated. Brains were excised, bisected in the midsagittal plane, and one hemisphere immersion-fixed in 4% paraformaldehyde/0.1M phosphate buffer (PB; pH 7.2) overnight at room temperature (RT). Within 24 h, the brains were rinsed with PB and dehydrated in ethanol, embedded in paraffin, and sections were cut at 8 μm. For unbiased stereology and immunostaining, mice from each treatment and age group were deeply anesthetized by Nembutal (52 mg/kg, i.p.) at 48 h post-injection of saline or TMT and perfused transcardially with 4°C 0.1 M phosphate buffer (PB) followed by 10 ml of 4°C 4% paraformaldehyde (PFA)/PB (ph 7.4). Brains post-fixed with 4% PFA/PB for 18 h, cryoprotected in 30% sucrose/PB, and frozen. Serial cryostat sections (≈70) were cut at an instrument setting of 50 μm through the entire hippocampus. Based upon sampling requirements for unbiased stereology, one section was selected from each block of 8 sections and stained for Nissl to visualize neuronal architecture.

2.4. Histological assessment of neuronal death

From each mouse, six H&E stained sections at systematic-random location were selected and the severity of dentate granule cell death scored by three independent observers according to an *a priori* defined severity scale (0-4), as previously described (Harry et al., 2008). Apoptotic cell death was detected with immunostaining for fractin, the product of beta actin cleavage by active caspase 3 (Oo et al., 2002). Sections were incubated (72 h at 4°C) in 0.3% Triton X-100, 2% normal goat serum, and rabbit polyclonal antibody to fractin (1:500; Invitrogen), rinsed, then incubated in 0.1M PB containing 0.3% Triton X-100, 2% normal goat serum and AlexaFluor® goat anti-rabbit 594 (1:500; Invitrogen) for 30 min at RT. Sections were coverslipped with ProLong Gold® with DAPI (Invitrogen). Digitized images of were acquired using a Leica LSM 5 laser-scanning microscope.

2.5. Immunohistochemistry for microglia and astrocyte response

Cryostat sections were incubated (72 h at 4°C) in 0.3% Triton X-100, 2% normal goat serum, and either rabbit polyclonal antibody to rabbit polyclonal anti-ionized calcium-binding adaptor molecule 1 (Iba1 1:500; Wako Chemicals, Japan) or GFAP (1:500; Dako Corp., Carpenteria, CA). Sections were washed, incubated in AlexaFluor® goat anti-rabbit 594 (1:500; Invitrogen) as described above. Sections were coverslipped with ProLong Gold® with DAPI (Invitrogen) as a nuclear counterstain. Digitized images were acquired using a Leica LSM 5 laser-scanning microscope.

2.6. Immunofluorescent staining and unbiased stereology of BrdU+ cells within the GCL/SGZ

Mice, at both ages, were injected with 5-bromo-2′-deoxyuridine (BrdU [50 mg/kg i.p]; Sigma-Aldrich, St. Louis, MO) at the time of TMT or saline dosing, and four injections thereafter every 12 h for 48 h allowing for incorporation at discrete intervals during the peak interval of NPC proliferation. Based upon sampling requirements for unbiased stereology, from the ~70 sagittal cryostat sections representing the entire hippocampus, a set of 8 sequential sections was sampled in a systemic-random manner, i.e., every eighth section with a random start on sections 1-8. Sections were incubated at 37°C in 1N HCL for 30 min, washed in PBS (30 min), and incubated in 0.1M PB with 0.3% Triton X-100, 2% normal goat serum and rat monoclonal antibody to BrdU (1:500; Accurate Biochemicals; Westbury, NY). Sections were washed, incubated in AlexaFluor® goat rat-488 (1:500; Invitrogen) as previously described, and coverslipped with ProLong Gold® with DAPI. Digitized images of immunofluorescence were acquired using a Leica DMBRE laser-scanning microscope.

To determine the number of newly generated BrdU+ cells, a fractionator, sampling scheme for rare events was used (Kempermann et al., 2002). The sum of objects counted was multiplied by the reciprocal of the fraction of reference space sampled. The sampling fractions were defined as follows: (a) section sampling fraction (ssf), the number of sections sampled divided by the total number of sections for each hippocampus; (b) area sampling fraction (asf), the area of the sampling frame divided by the area of the x-y sampling step; and (c) thickness sampling factor (tsf), the height of the dissector divided by the section thickness. BrdU+ cells co-stained with DAPI were identified throughout the latero-medial extension of the GCL and SGZ under 100× using a Leica DMRBE fluorescent microscope. In this procedure, the uppermost and lowermost 5 μm focal planes of the section were eliminated to avoid artifacts created by the knife blade. The number of BrdU+ cells was estimated as $N = \sum Q^- (1/\text{ssf})(1\text{asf})(1\text{tsf})$, where N = number of total estimated BrdU+ cells and $\sum Q^-$ = the number of counted BrdU+ cells. All analysis was conducted with the observer blinded to the treatment conditions.

2.7. Confirmation of immature NPC phenotype in BrdU+ cells by nestin immunofluorescent staining

A set of three sections was selected out of ~70 sagittal cryostat sections at random from animals in each age and treatment group. Sections were immunostained for BrdU as described with the addition of rabbit polyclonal anti-nestin (1:500; Abcam, Cambridge, MA) as a marker for immature NPCs. Immunoreactive product was detected with AlexaFluor® goat rat- 488 and AlexaFluor® goat rabbit-594 (1:500; Invitrogen) secondary antibodies. Sections were coverslipped with Prolong Gold® with DAPI. Digital images were acquired throughout the latero-medial extension of the GCL and SGZ under 60× magnification using a Leica LSM 5 laser-scanning microscope. A series of 1 mm sections throughout the entire z-plane was analyzed. To ensure that all nestin+ cells were captured regardless of location within the hippocampal dentate, either the GGL or the SGZ, cells were counted across both regions and data was expressed as the total number of BrdU+ cells co-expressing nestin.

2.8. qRT-PCR of hippocampal glial activation and pro-inflammatory cytokines

Total RNA was isolated from the hippocampus (n=6) using the RNeasy® Mini Kit (Qiagen, Valencia, CA) and 2.5 μg used for reverse transcription (SuperScript™II Reverse Transcriptase; Invitrogen). Quantitative real-time PCR (qRT-PCR) was carried out on a Perkin Elmer ABI Prism™ 7700 Sequence Detector using 3 μl cDNA as a template, combined with a reaction mixture to give final concentrations of 1X Power SYBR® Green Master Mix (Applied Biosystems; Foster City, CA) and optimized forward and reverse primers (Table 1). The 50 μl reaction mixtures were held at 50°C for 2 min, 95°C for 10 min, followed by 40 cycles at 95°C for 15 s, and 1 min at 60°C. Amplification curves from individual qRT-PCR reactions were generated (Sequence Detection System (SDS) 1.9.1 software (Applied Biosystems)). Relative mRNA amounts were calculated using a normalized standard curve and expressed as ratios of target gene to GAPDH.

2.9. Laser capture microdissection (LCM) of the SGZ

Cryostat sagittal brain sections (12 μm) were collected on uncoated glass slides and fixed for 1 min in 70% ethanol. Sections were rinsed in RNase-free water for 30 s, stained with Histogene® Staining Solution (Arcturus, Mountain View, CA) for 15 s, rinsed in RNase-free water for 30 s, dehydrated in 95% ethanol for 30 s, 100% ethanol for 30 s and xylene for 5 min, and air-dried for 5 min in a laminar flow hood. A two-cell width at the inner-blade edge of the GCL, representative of the SGZ, was excised using a PixCell Laser Capture Microscope with an infrared diode laser (Arcturus) within 2 h of cryosectioning. A total of 100 sections from each brain hemisphere provided $60000 \ \mu m^2 \times 100$ total area from the SGZ using 7500 laser pulses, 15 μm beam diameter, 75 mW power, 2.5 ms pulse. Total RNA from LCM samples was isolated on an individual animal basis (n = 6) using the PicoPure® RNA Isolation Kit (Arcturus) within 12 h of cyrosectioning. RNA on the column was subjected to RNase-Free DNase Set (Qiagen) then eluted with Elution Buffer. qRT-PCR was conducted as described for hippocampal tissues.

2.10. Generation of Primary Neurospheres

Two mm thick coronal sections containing the hippocampus were collected from three 21 day-old or 1 yr-old mice, as previously described (Bull and Bartlett, 2005). The hippocampus was dissected from the coronal slice excluding the corpus callosum, lateral ventricle, and cortex. Minced tissue was dissociated using the NeuroCult® Enzymatic Dissociation Kit for Adult Mouse and Rat CNS Tissue (Stemcell Technologies, Vancouver, BC). Single cell suspensions were sequentially filtered through 70 μm and 40 μm strainers into proliferation medium (PM) consisting of mouse NeuroCult® NSC Basal Medium (mouse) plus NeuroCult® NSC Proliferation Supplement (Stemcell Technologies) with the

addition of 20 ng/mL recombinant human epidermal growth factor (rhEGF), 10 ng/mL recombinant human fibroblast growth factor basic (rhFGFb), and 2 μg/mL heparin (StemCell Technologies). Single cell suspensions were plated at a density of 3500 cells/cm^2 in T-75 tissue culture flasks (BD Falcon) in PM, and incubated at 37°C in 5% CO_2/5% O_2, forming neurospheres by 7 days *in vitro* (DIV).

2.10.1. Neural colony forming-cell assay (NCFCA)—The NeuroCult® Neural Colony-Forming Cell Assay Kit (NCFCA; StemCell Technologies) was used to discriminate between stem and progenitor cells on the basis of their proliferative capability and size of colony formed. At 7 DIV, neurospheres generated from the hippocampus of each age and each dosing group were dissociated into single cell suspensions (NeuroCult® Chemical Dissociation Kit; StemCell Technologies) for use in NCFCA as previously described (Louis et al., 2008). Briefly 2.5×10^3 cells were plated in 35 mm tissue culture dishes in a semi-solid collagen matrix containing NeuroCult® NCFC media, supplemented with 20 ng/ml rhEGF, 10 ng/ml rhFGFb and 2 μg/ml heparin. Cultures were incubated at 37°C in 5% CO_2/5% O_2 and fed with 60 μl of PM every 7 days, until 21 days. At 21 days post-plating, the total number of colonies was counted from each experimental group, and categorized by size, as imaged by an inverted Nikon TE-2000 microscope using a 2 mm × 2 mm gridded scoring dish (StemCell Technologies).

2.10.2. qRT-PCR for IL-1R1, IL-1RAcP, IL-6Rα, gp130 in neurospheres—To measure mRNA expression, total RNA was isolated from neurospheres at 7 DIV (RNeasy® Mini Kit; Qiagen). qRT-PCR for each transcript (Table 1) was conducted as described for hippocampal samples. Amplification curves were generated and relative mRNA amounts were calculated using a normalized standard curve and expressed as ratio of target gene to GAPDH.

2.11. NCFCA in the presence of IL-1α or IL-6

The NCFCA was used to determine the effects of IL-1α or IL-6 on the formation of neural cell colonies. Based upon previous work (Harry et al., 2002; Monje et al., 2003) a dose range of recombinant IL1α and IL-6 was selected. At initial plating of single cell suspensions, media (NeuroCult® NCFC Serum Free Media without Cytokines; 20 ng/ml rhEGF, 10 ng/ml rhFGFb and 2 μg/ml heparin) was supplemented with either recombinant mouse IL-6 (rmIL-6, [5, 10, or 15 ng/ml]) or recombinant mouse IL-1α (rmIL-1α [75, 150, or 150 pg/ml]) (R&D Systems; Chicago, IL). In NPCs obtained from adolescent hippocampus, a linear dose response pattern was evident with a stimulation of proliferation observed with IL-1α and an inhibition with IL-6 (Suppl. Fig. 1). From this dose response, dose levels of IL-1α (150 pg/ml) and IL-6 (10ng/ml) were selected for a direct comparison of proliferation across age of NPCs. An additional comparison was conducted with a combined dosing of rm IL-6 [10 ng/ml and rm IL-1α [150 ng/ml]. Cells were incubated at 37°C in 5% CO_2/5% O_2. Cultures were fed with 60 μl of PM every 7 days until 21 days. At 21 days post-plating, the total number of colonies was counted from each experimental group, and categorized by size.

2.12. Statistical analysis

Data for cell number determination and each mRNA transcript displaying a homogenous distribution of variance were analyzed by ANOVA. Group differences between 21 day-old and 1 year-old mice with and without TMT were assessed using a 2 × 2 multi-factorial ANOVA with age and treatment as major factors. Subsequent independent group mean comparisons were conducted using the Bonferroni test. Student t-tests were conducted to determine the effect of combined cytokine exposure and mRNA levels within NPCs

obtained from control mice at each age. All statistical significance levels for independent group mean analyses were set at p < 0.05.

2.13. Microarray analysis

To examine changes induced in genes related to the IL-1 and IL-6 pathways, total RNA(10-20 ng) from LCM samples of the SGZ (n=3) was amplified (Affymetrix One-Cycle cDNA Synthesis Protocol). Fifteen μg of amplified biotin-cRNAs were fragmented and hybridized to Affymetrix Mouse Genome 430 2.0 GeneChip® array for 16 h at 45°C in a rotating hybridization oven using the Affymetrix Eukaryotic Target. Slides were stained with steptavidin/phycoerythrin using a double-antibody staining procedure and washed utilizing the EukGE-WS2v5 protocol of the Affymetrix Fluidics Station FS450 for antibody amplification. Arrays were scanned with an Affymetrix Scanner 3000 and data obtained using the GeneChip® Operating Software (GCOS; Version 1.2.0.037). Data were processed with an Affymetrix-specific error model for estimating measurement variance, using Rosetta Resolver, as described (Weng et al., 2006). Biological replicates were combined through error-weighted averaging and comparison ratios were built between samples. Statistical significance was set at p<0.001 and a minimum fold change of 1.2 was set as criteria.

Genes that were differentially regulated in 21 day-old versus 1 yr-old TMT exposed mice, taking into account differences in baseline expression in naïve mice, were analyzed using PathwayArchitect (Stratagene) software. This software uses the KEGG, DIP, and BIND databases and natural language scans of Medline to identify functional associations among differentially expressed genes. Gene interactions and associations (binding, expression, metabolism, promoter binding, protein modification and regulation) were represented graphically as a network. In this analysis, age was considered a mediator of injury related differential expression patterns using ANOVA.

3. Results

3.1. TMT induced an equivalent level of localized dentate granule neuron apoptosis at 21 days and 1 yr of age

We examined severity of neuronal apoptosis in the GCL and determined a uniform level and timing of hippocampal neuronal death induced by TMT across both ages. No evidence of cell death was observed by H&E staining in saline treated control (severity scores = 0-1; Fig. 1A,B). At 48 h post-TMT, dentate granule neurons displayed nuclear pyknosis and karyolysis (severity scores = 3-4; Fig. 1C,D). No indication of apoptosis was detected in saline control mice by immunostaining for fractin (Fig. 1E,F); fractin+ neurons were prominent following TMT (Fig. 1G,H).

3.2. TMT injury-induced proliferation is greater in the adolescent versus mature hippocampus

In the 21 day-old and 1 yr-old control mice, BrdU+ cells were sparse and restricted to the GCL inner blade/SGZ (Fig. 2A,B). An increase in BrdU+ cells was observed at 48 h post-TMT in the SGZ, as well as within the GCL in both 21 day-old (Fig. 2C) and the 1 yr-old mice (Fig. 2D). These visual observations were confirmed by unbiased stereology (Fig. 2E). Two-way ANOVA revealed a significant effect of treatment ($F_{(1,8)}$=49.58; p=0.0001), age ($F_{(1,8)}$=43.43; p=0.0002), and treatment × age interaction on BrdU+ cell number in the GCL/SGZ ($F_{(1,8)}$=27.20; p=0.0008). The number of BrdU+ cells within the GCL/SGZ was significantly higher in the 21 day-old control mice than in 1 yr-old control mice (p<0.05). In both age groups, TMT exposure resulted in a significant increase in the number of BrdU+ cells within the GCL/SGZ (p<0.05). In 21 day-old mice, the increase in BrdU+ cells was

approximately 7-fold higher than the basal level observed in controls. In 1 yr-old mice, the increase in BrdU+ cells was significantly less, at an estimated 3.5-fold elevation ($p<0.05$).

We then confirmed the proliferation of NPC by examining immunostaining for nestin and co-localization with BrdU (Fig. 2F-H). To capture any changes in the distribution of NPCs as a function age or injury, the distribution of BrdU+ cells across the entire GCL was examined. The percent total #BrdU+ cells throughout the GCL that co-expressed nestin was determined within controls and TMT-dosed mice for each age group (Fig. 2I). A two-way ANOVA indicated a significant main effect of age ($F_{(1,8)}=36.41$; $p=0.0003$) with the 21 day-old mice showing a higher percentage of co-localized immunostaining as compared to 1 yr-old, across both conditions. A significant main effect of TMT treatment ($F_{(1,8)}=49.04$; $p=0.0001$) was observed with an increase in co-localization at 48 h following TMT injection. No significant interaction of age and TMT was detected with the adolescent mice showing an approximate 30% increase over the higher basal level and the mature mice demonstrating an approximate 50% increase over the lower basal level.

3.3. Microglia demonstrate different morphological responses to injury as a function of age

In the normal 21 day-old mouse hippocampus, microglia displayed thin, ramified processes within the SGZ, hilus, and the densely packed dentate GCL (Fig 3A). Similar to the Iba-1 staining pattern in the 21 day-old, microglia within the 1 yr-old hippocampus were prominent within the hilus and molecular layer. In addition, Iba-1+ microglia displayed an increased staining in processes within the SGZ, hilus, and GCL (Fig. 3B), suggestive of a lower threshold for activation (Sparkman and Johnson, 2008).

In the 21 day-old mice, neuronal injury and loss following TMT induced an activation of microglia displaying an amoeboid morphology within proximity to dying neurons showing dense collapsed nuclei (Fig. 3C). In addition, process-bearing responsive microglia were evident throughout the GCL and in the hilus, occasionally extending into the SGZ. In 1 yr-old mice, a comparable level of neuronal death did not result in the localization of amoeboid microglia with dying neurons. Rather, prominent reactive microglia within the GCL displayed thick ramified processes. Similar to the 21 day-old mice, process-bearing reactive microglia were observed throughout the GCL and hilus occasionally extending into the SGZ (Fig. 3D). The morphological response of microglia was supported by qRT-PCR of Iba-1 (Fig. 3E). Two-way ANOVA of Iba-1 mRNA levels revealed a significant effect of treatment ($F_{(1,20)}=8.438$; $p<0.0088$) and higher levels seen in the 21 day-old TMT dosed mice. ($p<0.05$). No significant main effects of age or interaction between age and treatment were observed.

3.4. GFAP+ astrocytes demonstrate similar morphological responses to injury across ages

In control mice, minimal differences in GFAP staining were observed as a function of age. At both ages, astrocytes displayed fibrous processes projecting thorough the SGZ and GCL (Fig. 3F,G). Within 48 h post-TMT a retraction and moderate thickening of GFAP processes, was evident throughout the GCL (Fig. 3H,I). The increase in GFAP immunoreactivity with TMT was supported by qRT-PCR for GFAP mRNA levels (Fig. 3J). Two-way ANOVA revealed a significant effect of treatment ($F_{(1,20)}=14.82$; $p=0.001$) with a significant increase observed following TMT in both ages, as compared to controls ($p<0.05$). No significant main effects of age or age × treatment interaction were observed.

3.5. IL-1α and IL-6 mRNA levels are differentially elevated in the hippocampus following TMT as a function of age

Given the differential activation of microglia in 21 day-old, as compared to 1 yr-old mice, additional characterization of the microglial response was conducted based on proposed pro-inflammatory (MI) or anti-inflammatory (M2) phenotypes (Colton and Wilcock, 2010; Michelucci et al., 2009). Gene expression associated with the M1 phenotype was examined (IL-1β, IL-6) as well as the pro-inflammatory cytokine IL-1α. Expression of anti-inflammatory M2 phenotype associated genes: arginase I (AG-I), chitinase 3-like-3 (YM-1), IL-10, and transforming growth factor beta (TGFβ1) were also examined. Consistent with our previous work (Bruccoleri et al., 1998), we did not observe an elevation in mRNA levels for TGFβ1 in the hippocampus at this early time point (Fig. 4A). IL-10 and AG-I mRNA levels were not significantly altered in the hippocampus (Fig. 4A) following TMT. No signal for YM-1 mRNA was detected (data not shown). IL-1β mRNA expression was not significantly elevated by TMT in either age group (Fig. 4A). Two-way ANOVA for IL-1α mRNA expression showed significant main effects of treatment ($F_{(1,20)}=45.41$; $p=<0.0001$), age ($F_{(1,20)}=19.91$; $p<0.0001$), and treatment × age interaction ($F_{(1,20)}=24.67$; $p=<0.0001$). A significant TMT-induced elevation was observed in 21 day-old mice ($p<0.001$). IL-6 mRNA levels in the hippocampus were significantly elevated following TMT ($F_{(1,20)}=7.755$; $p=<0.05$) in 1 yr-old mice ($p<0.001$).

3.6. TMT-induced injury selectively elevated IL-6 mRNA in SGZ of mature mice

To further examine whether the differential inflammatory cytokine response observed in the hippocampus was observed within the SGZ, mRNA levels were determined from LCM samples. A slight elevation in mRNA levels for TGFβ1 within the SGZ following TMT was noted at both ages but failed to reach statistical significance (Fig. 4B). IL-10 and AG-I mRNA levels in the SGZ were not significantly altered by TMT (Fig. 4B). No signal for YM-1 mRNA was detected (data not shown). mRNA levels for IL-1β showed no significant differences as a function of age or TMT injection (Fig. 4B). IL-1α mRNA levels (Fig. 4B) were significantly elevated with TMT ($F_{(1,20)}=42.50$; $p<0.0001$) in both age groups ($p<0.01$). No significant effect was observed as a function of age. IL-6 mRNA levels (Fig. 4B) were significantly elevated by TMT ($F_{(1,20)}=8.595$; $p<0.005$) and with age ($F_{(1,20)}=5.304$; $p<0.05$). A significant treatment × age interaction ($F_{(1,20)}=5.036$; $p<0.05$) was detected with TMT-induced elevations in IL-6 mRNA levels occurring in 1 yr-old mice ($p<0.05$).

3.7. *In vivo* TMT exposure induced neural colony cell formation *in vitro*

Neurogenic cells within the SGZ are primarily progenitor cells that maintain the capability to differentiate into neurons or glia (Bull and Bartlett, 2005; Seaberg and van der Kooy, 2002); however, with localized neuronal activation, a latent stem cell population has also been identified (Walker et al., 2008). Using the NCFCA to discriminate between colonies of neural stem and progenitor cells, we examined alterations in the size of colonies formed from hippocampal cells as a function of age and *in vivo* neuronal activation/injury by TMT. We found no difference in culturing success of NPC from young and mature brains, consistent with similar published work (Blackmore et al., 2009). Colonies >2.0 mm were not observed in either age or treatment group, suggesting origination from progenitor cells, rather than stem cells. The mean total number of colonies generated *in vitro* was greater in 21 day-old as compared to the 1 yr-old saline control mice (Fig. 5A; p<0.005). TMT treatment induced colony formation from both 21 day-old and 1 yr-old mice. The number of colonies generated from the hippocampus of mice injected with TMT was greater at 21 days of age compared to the 1 yr-old; however, the fold increase over saline control was similar in both ages (1.8 fold for 21 day-old and 1.9 fold for the 1 yr-old).

3.8. NPCs from the adolescent and mature hippocampus express IL-1R1, IL-1RAcP, IL-6Rα, and gp130

To confirm that NPC displayed the capability to respond to the *in vivo* elevations in IL-1α and IL-6 within the SGZ, IL-1R1, IL-1RAcP, IL-6Rα, and gp130 mRNA levels were determined in isolated NPCs generated from each age group. A basal level of each transcript was detected (Fig. 5D). No differences as a function of age were seen for IL-1R1, IL-1RAcP, or gp130. Hippocampal NPCs derived from 1 year-old mice expressed higher levels of IL-6Rα, compared to NPCs from 21 day-old mice (t = 4.871, $p < 0.05$).

3.9. IL-1α stimulated colony formation of adolescent NPCs and IL-6 inhibited colony formation of adolescent and mature NPCs

Given the expression of IL-1 and IL-6 receptors on NPCs, we examined the proliferative response to exogenous recombinant IL-1α, IL-6, or a combination of IL-1α and IL-6 proteins in the NCFCA. Following a 21 DIV exposure to rmIL-1α, two-way ANOVA revealed a significant effect of treatment ($F_{(1,8)}=14.64$; $p=0.005$), age ($F_{(1,8)}=127.3$; $p=<0.0001$), and treatment × age interaction on total colony formation ($F_{(1,8)}=7.029$; $p=0.02$). Treatment with rmIL-1α significantly increased formation of colonies obtained from the hippocampus of 21 day-old mice ($p<0.05$; Fig. 6A). rmIL-1α did not stimulate colony proliferation in cultures obtained from the hippocampus of 1 yr-old mice. Following 21 DIV, exposure to rmIL-6 produced a significant effect of treatment ($F_{(1,8)}=14.64$; $p=0.005$), age ($F_{(1,8)}=127.3$; $p=<0.0001$), and treatment × age interaction on total colony formation ($F_{(1,8)}=7.029$; $p=0.02$). Decreased colony formation with rmIL-6 was observed in hippocampal NPC from both ages ($p<0.05$; Fig. 6B). In NPCs from 21 day-old mice, concurrent exposure to IL-1α and IL-6 did not result in a significant increase in colony formation thus, inhibiting the stimulatory properties of IL-1α. (Fig. 6C) In NPCs from 1-yr-old mice, concurrent exposure to both cytokines resulted in a significant decrease (t=3.113, $p<0.05$) in colony formation similar to the effects observed with IL-6 alone.

3.10. Differential activation of the IL-1 pathway in the adolescent and the IL-6 pathway in the mature SGZ following TMT injury

Based upon our observations that hippocampal NPCs isolated from both age groups 1) expressed IL-1 and IL-6 receptors for downstream signaling activation, 2) expressed both cytokines *in vivo* within the SGZ, and 3) demonstrated age related proliferative responses in isolated NPC, we examined the molecular profiles associated with both receptor pathways as a function of age and injury. Microarray profiles generated from LCM SGZ tissue identified a total of 109 unique transcripts changed in the 21 day-old samples, 54 unique transcripts in the 1 yr-old samples, with a total of 88 similarly changed at both ages as a function of TMT (Fig. 7A). While a full analysis of the microarray data is outside the scope of this manuscript, a number of genes were identified in support of the speculation that a greater level of "immune" activation occurs in the adolescent SGZ. For example, CD44 antigen transcript was elevated 10.9-fold ($p<0.0001$) in the adolescent with only a 2-fold ($p=0.23$) elevation in the adult. Similar patterns were seen for Mmd (monocytes to macrophage differentiation-associated) transcripts with a 2.8-fold increase in the adolescent ($p<0.00001$) and a 1.4 fold increase in the adult ($p=0.0005$) and for Msr2 (macrophage scavenger receptor 2) with a 3.4-fold increase ($p<0.000001$) in the adolescent and a 1.08-fold non-significant increase in the adult.

We used PathwayArchitect software to examine the differential expression of IL-1α and IL-6 related genes in the SGZ as a function of age and TMT injury. The transcript expression pattern generated from the SGZ suggested a primary involvement with injury of the IL-1 signaling pathway in the 21 day-old mice with IL-6 serving a primary role in the SGZ of 1 yr-old mice (Fig. 7B). Using this approach, statistical significance was set at

p<0.001 and a minimum fold change of 1.2 was set as criteria. IL-1α and IL-1R1 were induced at a greater level in the adolescent SGZ compared with the mature SGZ. A specific alternative pathway for neurogenesis has yet to be reported. We now report a network association between IL-1α and signaling genes downstream of IL-1R1 including: myeloid differentiation primary response gene-88 (Myd88), IκB, and NFκB1 in the SGZ with higher levels in the 21 day-old injured SGZ as compared to the 1 yr-old mice.

With TMT injury, IL-6 mRNA levels were significantly elevated in the SGZ of 1 yr-old with a minimal induction in 21 day-old mice. The IL-6/IL-6R complex initiates signaling through the gp130 receptor (Jones et al., 2005) leading to activation of either Janus kinase (JAK) or Ras-mediated signaling (Heinrich et al., 1998; Hirano et al., 2000) regulating cell growth, proliferation, differentiation, and apoptosis. We noted a concurrent upregulation of IL-6 and a number of Ras-mediated signaling genes in the SGZ of adult mice following injury. Ras-Genes elevated in the Ras/MAPK signaling pathway included SHC, the gene encoding a signaling and transforming protein Src homology 2 and 3 that are involved in mitogenic signal transduction and facility the activation of Ras proteins. Growth factor receptor bound protein-2 (Grb-2), an adaptor protein involved in epidermal growth factor receptor tyrosine kinase for the activation of Ras and downstream kinases, ERK1,2. Elevations were noted in v-raf-1, murine leukemia viral oncogene homolog 1 (Raf-1), the gene encoding MAP3K that functions downstream of Ras membrane associated GTPases. Raf-1 phosphorylates MEK1 and MEK2 to activate ERK1 and ERK2, controlling gene expression involved in cell division, differentiation, migration, and apoptosis. Elevations were seen in mitogen-activate protein kinase kinase-1 (MAP2K1) for which the associated protein product, MEK1 protein kinase is essential for normal development before and survival after birth.

4. Discussion

In the current study, we examined microglia activation, IL-1α and IL-6 mRNA levels, and NPC proliferation within the SGZ in mice exposed to the hippocampal toxicant, TMT. Based upon the adolescent establishment of the proliferative SGZ (Schlessinger et al., 1975) and active NPC proliferation in the hippocampus, we further compared differences in the response to TMT-induced injury as a function of age. These comparisons incorporated differences in the SGZ of the normal adolescent hippocampus as compared to an adult age showing a decline in NPC proliferation. Our data confirmed previous reports of a greater number of NPCs in the SGZ of adolescent, as compared to adult mice under normal conditions (Ben Abdallah et al., 2010; He and Crews, 2007; Kuhn et al., 1996), as well as with brain injury (Hattiangady et al., 2008; Shetty et al., 2010). The novel findings of these studies include age-related differences in the response of isolated NPCs to IL-1α or IL-6 and the molecular profiles generated from the injured SGZ. First, we report that the age-related level of NPC proliferation *in vivo* following TMT-induced injury correlates with elevations in IL-1α mRNA levels in the adolescent hippocampus and IL-6 within the adult. We show that proliferation of NPCs isolated from the hippocampus of mice at both ages was inhibited by IL-6. Proliferation of NPCs by IL-1α was observed only in cells derived from the hippocampus of adolescent mice and not from NPCs from the mature hippocampus. Third, we examined the molecular profile of the SGZ from each age and treatment and identified distinct signaling pathway activations as a function of age. TMT injury selectively induced an activation of IL-1α signaling via IL-1R1 and downstream genes within the IkB/NFkB1 signaling pathway in the 21 day-old and IL-6Rα/gp130 signaling via the Ras/MAPK pathway in the 1 yr-old mice. From these data, we conclude that the age related expression of IL-1α and subsequent signaling pathway activation in the adolescent fosters NPC proliferation. In comparison, activation of the IL-6Rα/gp130 pathway in the adult

contributes to maintaining a tight regulatory control on NPC proliferation, thus serves as a basis for an age-dependent level of NPC self-renewal following injury.

Both IL-1β and IL-α induce signaling via binding to IL-R1 followed by a sequence of protein-protein interactions forming a complex to recruit IL-1RAcP (Greenfeder et al., 1995). Myeloid differentiation primary response gene-88 (Myd88) is then recruited to the IL-1α/IL-R1 complex activating the interleukin-1 receptor associated kinase (IRAK) (Wesche et al., 1997), for activation either of ERK, p38MAPK, c-jun, or NFκB signaling (Dunne and O'Neill, 2003; O'Neill, 2002; O'Neill and Greene, 1998). Previous studies have demonstrated that IL-1R1 is expressed *in vitro* in NPCs isolated from the rat embryonic forebrain (Wang et al., 2007) and in the adult rat hippocampus *in vivo* (Koo and Duman, 2008). This receptor expression suggests the potential for direct effect of receptor action via IL-1β or IL-1α (Greenfeder et al., 1995). Wang et al., (2007) demonstrated that the treatment of rat embryonic forebrain NPCs with IL-1β and upon IL1-R1 activation of the SAP/JNK pathway inhibited proliferation. Additionally, activation of the NFκB pathway by IL-1β binding to IL-1R1 decreased proliferation but not differentiation of adult hippocampal NPCs both *in vivo* and *in vitro* (Koo and Duman, 2008). Inhibition of proliferation, observed by Wang et al. (2007), was accompanied by a normal pattern of cell differentiation; but a lower level of GFAP protein expression in differentiated NPCs. A direct effect of IL-1β on the differentiation of NPCs to neurons has been suggested by the work of Kuzumaki et al., (2010) indicating a decrease in β-tubulin+ neurons differentiated from mouse whole brain embryonic NPCs.

While the majority of the work on IL-1 signaling in NPCs has focused on IL-1β, IL-1α also activates the IL-1R1 and direct effects on NPCs have been observed. Using mouse embryonic cortical NPCs, IL-1α exposure was reported to direct differentiation to the astrocyte lineage (Ajmone-Cat et al., 2010). The effect of IL-1R1 signaling on NPC proliferation has been supported by the studies of Spulber et al. (2008) utilizing transgenic mice overexpressing IL-1 receptor antagonist (IL-1ra). In these animals, the overexpression of IL-1ra was sufficient to inhibit *in vivo* excitotoxicity-induced hippocampal progenitor cell proliferation. Further observations from this study suggested that the effect of IL-1ra on the *in vivo* basal level of hippocampal progenitor cell proliferation was influenced by the age of the animal. In 5 month-old mice, the IL-1ra transgenic mice demonstrated a decrease in basal proliferation for which no such effects were observed in mice at ~22 months of age. Our current data supports the work of Spulber et al. (2008) suggesting that the effect of IL-1R1 activation on NPCs can be dependent upon the age of the animal. In the isolated SGZ, a significant elevation was observed for IL-1α in both age groups; however, activation of the IkB/NFkB signaling cascade was restricted to the adolescent. Consistent with this *in vivo* observation, IL-1α stimulated *in vitro* proliferation of NPCs isolated from adolescent hippocampus; while, no such effects were observed in cells isolated from the adult. Activated microglia provide the earliest source of IL-1α and IL-1ra after injury (Eriksson et al., 2000; Eriksson et al., 1999) and in the TMT-induced injury model (Bruccoleri et al., 1998). Thus, the age related changes we observed in the current study with regards to IL-1R1 activation are likely influenced by the maturation of microglia and differences in activation. Just as the functional capability of microglia change in the aged brain (Streit, 2006), microglia during the postnatal period represent a more immature phenotype (Kuzumaki et al., 2010; Rezaie and Male, 1999; Yokoyama et al., 2004). TMT induced a similar severity of neuronal death in both age groups but a pronounced activation of microglia within the GCL was seen only in the adolescent, as evidenced by the morphological phenotype and the elevation in IL-1α. In the adult, a more blunted hypertrophic process-bearing microglia response was observed. No elevation was observed the in microglia M2 associated genes, AG-I, TGFβ1, IL-10, and chitinase-3-like-3 (YM-1) (Colton and Wilcock, 2010; Michelucci et al., 2009) suggesting the absence of an

alternatively activated microglia phenotype at both ages following TMT exposure. Thus, as a source of IL-1α in this injury model (Bruccoleri et al., 1998), activated microglia could serve as a major influence not only on the NPC *in vivo* but also on the surrounding astrocytes, resulting in an environment promoting differences observed as a function of age.

The prominent cytokine response observed in the adult GCL and SGZ following TMT-induced injury was the up-regulation of IL-6. We also showed a slight elevation in mRNA levels of IL-6 in the normal adult hippocampus as compared to the adolescent. This finding is consistent with the report of an increase in IL-6 protein expression in the hippocampus of aged, as compared to juvenile mice (Ye and Johnson, 1999,2001). While a body of literature exists demonstrating the ability of multiple neural cell types to express IL-6 mRNA or protein, there is limited available data in the literature demonstrating the cellular source of IL-6 within the brain. Recent work suggests the expression of IL-6 protein in cortical lesions from patients with either tuberous sclerosis complex (TSC) or focal cortical dysplasia type IIb (FCDIIb)(Shu et al., 2010). Within the TSC tubers cortical tubers, IL-6 immunoreactivity co-localized to dysmorphic neurons and giant neurons with no evidence of localization to GFAP astrocytes. In FCDIIb, balloon cells expressed both IL-6 and GFAP. Additional work suggests the expression of IL-6 in neurons of the cerebral cortex and hypothalamus with trinitrobenzene sulfonic acid-induced colitis (Wang et al., 2010). Further work has demonstrated that the combination of neuronal depolarization and activation of IL-1R1 with IL-1β can induce neurons to synthesize and release IL-6 (Juttler et al., 2002;Ringheim et al., 1995; Tsakiri et al., 2008a,b). It is possible that the production of IL-1α by microglia, coinciding with the stimulation of neurons by TMT, could lead to the increased neuronal production of IL-6. Microglial production of IL-6 has also been demonstrated in non-pathological conditions *in vivo* (Schobitz et al., 1992) and classically activated M1 microglia are also identified to produce IL-6 (Colton and Wilcock, 2010;Monje et al., 2003). We attempted to identify the cellular source of IL-6 within the current study however, a consistent staining pattern was not observed across various antibody sources. With a monoclonal antibody we were able to identify localization to neurons; yet, with a polyclonal antibody, a similar pattern of neuronal expression was lacking and the overall impression was of localization to microglia. In neither case did we identify immunoreactivity within GFAP+ astrocytes. However, to identify the cellular source will require additional studies to verify specificity of the antibodies and confirmation of a consistent pattern of immunostaining. Whatever the source, the effects of IL-6 upon NPCs were clearly demonstrated.

IL-6 binds to IL-6Rα then to the gp130 receptor to initiate signal transduction via the Janus tyrosine kinase /signal transducers and activators of transcription 3 (JAK/STAT3) and phosphatidylinositol (PI)-3 kinase/Akt pathways. It is known that these pathways can then be employed as a mechanism for cell survival (Reich, 2007). Recent studies report that, while rat embryonic neural stem cells respond *in vitro* to IL-6 (Nakanishi et al., 2007), NPCs from the embryonic subventricular zone (SVZ) do not express a functional membrane IL-6R (Islam et al., 2009). In this latter case, exposure to hyper IL-6 (the complex of IL-6/IL-6R) was required to stimulate gp130 signaling and cell differentiation (Islam et al., 2009). IL-6 has been shown to promote astrocytic differentiation of embryonic neural stem cells derived from the rat SVZ (Nakanishi et al., 2007) via the Janus tyrosine kinase/signal transducers and activators of transcription 3 (JAK/STAT3) signaling pathway (Bromberg and Darnell, 2000). Monje et al., (2003) reported that, *in vitro*, IL-6 inhibits neuronal differentiation of adult hippocampal NPCs; however, recent work demonstrated that while gliogenesis due to IL-6 receptor activation is related to signaling via the JAK/STAT pathway, neuronal differentiation occurs via activation of the RAS-MAPK signaling pathway (Islam et al., 2009; Taga and Fukuda, 2005). Within the SGZ of the adult brain, we now report elevations in genes associated with both IL-6Rα and gp130, as well as genes associated with

downstream signaling through Ras to activate Raf-1 or MAP2K1. The prevailing hypothesis that acute exposure to IL-6 is detrimental to NPCs (Ekdahl et al., 2003; Ekdahl et al., 2009; Monje et al., 2003; Vallieres et al., 2002), is further supported by our finding that IL-6 inhibited proliferation of hippocampal NPCs, regardless of age. While the inhibition of proliferation may be a direct effect, further studies may determine a correlation with an earlier onset of differentiation. In light of the work of Islam et al. (2009), a possible role for IL-6 in promoting neurogenesis for replacement of dentate granule cells following hippocampal injury with TMT requires consideration.

In the early work identifying the sustained neuro-proliferative capability of the hippocampus, Altman et al., (1973) proposed the idea that changes occurring with maturation from the adolescent to the adult hippocampus represented selective stabilization of the structure. Consistent with this idea, and similar ones proposed by Changeux and Dauchin (1976), is the idea that the higher levels of NPC proliferation observed in the adolescent brain reflect a greater level of hippocampal plasticity. Lower levels observed in the adult appear to reflect a system focused on maintaining cellular homeostasis and survival. We now propose that the contribution of pro-inflammatory cytokines, and possibly neuroinflammation in general, varies as a function of maturational stage and can assume different regulatory roles with regards to the self-renewal of NPCs within the injured hippocampus. One could speculate that the upregulation of IL-1α, as an initiator, and the lack of corresponding upregulation of IL-6, as a down-regulator, serve to enhance the neurogenic proliferative response to injury in the adolescent SGZ. In comparison, in the adult hippocampus, the GCL is a more developed and compacted region and the induction of IL-6 and absence of IL-1 signaling with injury may represent these maturational differences. The dynamic neurogenic response in the adolescent hippocampus following the death of dentate granule neurons as a result of a systemic injection of TMT provides a model to identify critical factors delineating the adolescent SGZ and the transition to an adult profile.

Supplementary Material

Refer to Web version on PubMed Central for supplementary material.

Acknowledgments

References

Aberg MA, Aberg ND, Hedbacker H, Oscarsson J, Eriksson PS. Peripheral infusion of IGF-I selectively induces neurogenesis in the adult rat hippocampus. J Neurosci. 2000; 20:2896–2903. [PubMed: 10751442]

Ajmone-Cat MA, Cacci E, Ragazzoni Y, Minghetti L, Biagioni S. Pro-gliogenic effect of IL-1alpha in the differentiation of embryonic neural precursor cells in vitro. J Neurochem. 2010; 113:1060–1072. [PubMed: 20236219]

Alvarez-Buylla A, Lim DA. For the long run: maintaining germinal niches in the adult brain. Neuron. 2004; 41:683–686. [PubMed: 15003168]

Banasr M, Hery M, Printemps R, Daszuta A. Serotonin-induced increases in adult cell proliferation and neurogenesis are mediated through different and common 5-HT receptor subtypes in the dentate gyrus and the subventricular zone. Neuropsychopharmacology. 2004; 29:450–460. [PubMed: 14872203]

Ben Abdallah NM, Slomianka L, Vyssotski AL, Lipp HP. Early age-related changes in adult hippocampal neurogenesis in C57 mice. Neurobiol Aging. 2010; 31:151–161. [PubMed: 18455269]

Blackmore DG, Golmohammadi MG, Large B, Waters MJ, Rietze RL. Exercise increases neural stem cell number in a growth hormone-dependent manner, augmenting the regenerative response in aged mice. Stem Cells. 2009; 27:2044–2052. [PubMed: 19544415]

Bromberg J, Darnell JE Jr. The role of STATs in transcriptional control and their impact on cellular function. Oncogene. 2000; 19:2468–2473. [PubMed: 10851045]

Bruccoleri A, Brown H, Harry GJ. Cellular localization and temporal elevation of tumor necrosis factor-alpha, interleukin-1 alpha, and transforming growth factor-beta 1 mRNA in hippocampal injury response induced by trimethyltin. J Neurochem. 1998; 71:1577–1587. [PubMed: 9751191]

Bull ND, Bartlett PF. The adult mouse hippocampal progenitor is neurogenic but not a stem cell. J Neurosci. 2005; 25:10815–10821. [PubMed: 16306394]

Cacci E, Claasen JH, Kokaia Z. Microglia-derived tumor necrosis factor-alpha exaggerates death of newborn hippocampal progenitor cells in vitro. J Neurosci Res. 2005; 80:789–797. [PubMed: 15884015]

Cameron HA, Gould E. Adult neurogenesis is regulated by adrenal steroids in the dentate gyrus. Neuroscience. 1994; 61:203–209. [PubMed: 7969902]

Colton CA, Wilcock DM. Assessing activation states in microglia. CNS Neurol Disord Drug Targets. 2010; 9:174–191. [PubMed: 20205642]

Das S, Basu A. Inflammation: a new candidate in modulating adult neurogenesis. J Neurosci Res. 2008; 86:1199–1208. [PubMed: 18058947]

Davalos D, Grutzendler J, Yang G, Kim JV, Zuo Y, Jung S, Littman DR, Dustin ML, Gan WB. ATP mediates rapid microglial response to local brain injury in vivo. Nat Neurosci. 2005; 8:752–758. [PubMed: 15895084]

Dunne A, O'Neill LA. The interleukin-1 receptor/Toll-like receptor superfamily: signal transduction during inflammation and host defense. Sci STKE. 2003; 2003:re3. [PubMed: 12606705]

Ekdahl CT, Claasen JH, Bonde S, Kokaia Z, Lindvall O. Inflammation is detrimental for neurogenesis in adult brain. Proc Natl Acad Sci U S A. 2003; 100:13632–13637. [PubMed: 14581618]

Ekdahl CT, Kokaia Z, Lindvall O. Brain inflammation and adult neurogenesis: the dual role of microglia. Neuroscience. 2009; 158:1021–1029. [PubMed: 18662748]

Eriksson C, Nobel S, Winblad B, Schultzberg M. Expression of interleukin 1 alpha and beta, and interleukin 1 receptor antagonist mRNA in the rat central nervous system after peripheral administration of lipopolysaccharides. Cytokine. 2000; 12:423–431. [PubMed: 10857755]

Eriksson C, Van Dam AM, Lucassen PJ, Bol JG, Winblad B, Schultzberg M. Immunohistochemical localization of interleukin-1beta, interleukin-1 receptor antagonist and interleukin-1beta converting enzyme/caspase-1 in the rat brain after peripheral administration of kainic acid. Neuroscience. 1999; 93:915–930. [PubMed: 10473257]

Greenfeder SA, Nunes P, Kwee L, Labow M, Chizzonite RA, Ju G. Molecular cloning and characterization of a second subunit of the interleukin 1 receptor complex. J Biol Chem. 1995; 270:13757–13765. [PubMed: 7775431]

Harry GJ, Funk JA, d'Hellencourt C. Lefebvre, McPherson CA, Aoyama M. The type 1 interleukin 1 receptor is not required for the death of murine hippocampal dentate granule cells and microglia activation. Brain Res. 2008; 1194:8–20. [PubMed: 18191113]

Harry GJ, Lefebvre d'Hellencourt C. Dentate gyrus: alterations that occur with hippocampal injury. Neurotoxicology. 2003; 24:343–356. [PubMed: 12782100]

Harry GJ, McPherson CA, Wine RN, Atkinson K, d'Hellencourt C. Lefebvre. Trimethyltin-induced neurogenesis in the murine hippocampus. Neurotox Res. 2004; 5:623–627. [PubMed: 15111239]

Harry GJ, Tyler K, d'Hellencourt CL, Tilson HA, Maier WE. Morphological alterations and elevations in tumor necrosis factor-alpha, interleukin (IL)-1alpha, and IL-6 in mixed glia cultures following exposure to trimethyltin: modulation by proinflammatory cytokine recombinant proteins and neutralizing antibodies. Toxicol Appl Pharmacol. 2002; 180:205–218. [PubMed: 12009860]

Hattiangady B, Rao MS, Shetty AK. Plasticity of hippocampal stem/progenitor cells to enhance neurogenesis in response to kainate-induced injury is lost by middle age. Aging Cell. 2008; 7:207–224. [PubMed: 18241325]

He J, Crews FT. Neurogenesis decreases during brain maturation from adolescence to adulthood. Pharmacol Biochem Behav. 2007; 86:327–333. [PubMed: 17169417]

Heinrich PC, Behrmann I, Muller-Newen G, Schaper F, Graeve L. Interleukin-6-type cytokine signalling through the gp130/Jak/STAT pathway. Biochem J. 1998; 334(Pt 2):297–314. [PubMed: 9716487]

Hirano T, Ishihara K, Hibi M. Roles of STAT3 in mediating the cell growth, differentiation and survival signals relayed through the IL-6 family of cytokine receptors. Oncogene. 2000; 19:2548–2556. [PubMed: 10851053]

Islam O, Gong X, Rose-John S, Heese K. Interleukin-6 and neural stem cells: more than gliogenesis. Mol Biol Cell. 2009; 20:188–199. [PubMed: 18971377]

Jones SA, Richards PJ, Scheller J, Rose-John S. IL-6 transsignaling: the in vivo consequences. J Interferon Cytokine Res. 2005; 25:241–253. [PubMed: 15871661]

Juttler E, Tarabin V, Schwaninger M. Interleukin-6 (IL-6): a possible neuromodulator induced by neuronal activity. Neuroscientist. 2002; 8:268–275. [PubMed: 12061506]

Kaneko N, Kudo K, Mabuchi T, Takemoto K, Fujimaki K, Wati H, Iguchi H, Tezuka H, Kanba S. Suppression of cell proliferation by interferon-alpha through interleukin-1 production in adult rat dentate gyrus. Neuropsychopharmacology. 2006; 31:2619–2626. [PubMed: 16823390]

Kempermann G, Gast D, Gage FH. Neuroplasticity in old age: sustained fivefold induction of hippocampal neurogenesis by long-term environmental enrichment. Ann Neurol. 2002; 52:135–143. [PubMed: 12210782]

Koo JW, Duman RS. IL-1beta is an essential mediator of the antineurogenic and anhedonic effects of stress. Proc Natl Acad Sci U S A. 2008; 105:751–756. [PubMed: 18178625]

Kuhn HG, Dickinson-Anson H, Gage FH. Neurogenesis in the dentate gyrus of the adult rat: age-related decrease of neuronal progenitor proliferation. J Neurosci. 1996; 16:2027–2033. [PubMed: 8604047]

Kuzumaki N, Ikegami D, Imai S, Narita M, Tamura R, Yajima M, Suzuki A, Miyashita K, Niikura K, Takeshima H, Ando T, Ushijima T, Suzuki T. Enhanced IL-1beta production in response to the activation of hippocampal glial cells impairs neurogenesis in aged mice. Synapse. 2010

Larsson E, Mandel RJ, Klein RL, Muzyczka N, Lindvall O, Kokaia Z. Suppression of insult-induced neurogenesis in adult rat brain by brain-derived neurotrophic factor. Exp Neurol. 2002; 177:1–8. [PubMed: 12429205]

Lawson LJ, Perry VH, Dri P, Gordon S. Heterogeneity in the distribution and morphology of microglia in the normal adult mouse brain. Neuroscience. 1990; 39:151–170. [PubMed: 2089275]

Louis SA, Rietze RL, Deleyrolle L, Wagey RE, Thomas TE, Eaves AC, Reynolds BA. Enumeration of neural stem and progenitor cells in the neural colony-forming cell assay. Stem Cells. 2008; 26:988–996. [PubMed: 18218818]

Mathieu P, Battista D, Depino A, Roca V, Graciarena M, Pitossi F. The more you have, the less you get: the functional role of inflammation on neuronal differentiation of endogenous and transplanted neural stem cells in the adult brain. J Neurochem. 2010; 112:1368–1385. [PubMed: 20028453]

McPherson CA, Kraft AD, Harry GJ. Injury-Induced Neurogenesis: Consideration of Resident Microglia as Supportive of Neural Progenitor Cells. Neurotox Res. 2010

Michelucci A, Heurtaux T, Grandbarbe L, Morga E, Heuschling P. Characterization of the microglial phenotype under specific pro-inflammatory and anti-inflammatory conditions: Effects of oligomeric and fibrillar amyloid-beta. J Neuroimmunol. 2009; 210:3–12. [PubMed: 19269040]

Ming GL, Song H. Adult neurogenesis in the mammalian central nervous system. Annu Rev Neurosci. 2005; 28:223–250. [PubMed: 16022595]

Monje ML, Toda H, Palmer TD. Inflammatory blockade restores adult hippocampal neurogenesis. Science. 2003; 302:1760–1765. [PubMed: 14615545]

Mrak RE, Griffin WS. Glia and their cytokines in progression of neurodegeneration. Neurobiol Aging. 2005; 26:349–354. [PubMed: 15639313]

Nakanishi M, Niidome T, Matsuda S, Akaike A, Kihara T, Sugimoto H. Microglia-derived interleukin-6 and leukaemia inhibitory factor promote astrocytic differentiation of neural stem/progenitor cells. Eur J Neurosci. 2007; 25:649–658. [PubMed: 17328769]

Nimmerjahn A, Kirchhoff F, Helmchen F. Resting microglial cells are highly dynamic surveillants of brain parenchyma in vivo. Science. 2005; 308:1314–1318. [PubMed: 15831717]

O'Neill LA. Signal transduction pathways activated by the IL-1 receptor/toll-like receptor superfamily. Curr Top Microbiol Immunol. 2002; 270:47–61. [PubMed: 12467243]

O'Neill LA, Greene C. Signal transduction pathways activated by the IL-1 receptor family: ancient signaling machinery in mammals, insects, and plants. J Leukoc Biol. 1998; 63:650–657. [PubMed: 9620655]

Oo TF, Siman R, Burke RE. Distinct nuclear and cytoplasmic localization of caspase cleavage products in two models of induced apoptotic death in dopamine neurons of the substantia nigra. Exp Neurol. 2002; 175:1–9. [PubMed: 12009755]

Reich NC. STAT dynamics. Cytokine Growth Factor Rev. 2007; 18:511–518. [PubMed: 17683973]

Rezaie P, Male D. Colonisation of the developing human brain and spinal cord by microglia: a review. Microsc Res Tech. 1999; 45:359–382. [PubMed: 10402264]

Ringheim GE, Burgher KL, Heroux JA. Interleukin-6 mRNA expression by cortical neurons in culture: evidence for neuronal sources of interleukin-6 production in the brain. J Neuroimmunol. 1995; 63:113–123. [PubMed: 8550808]

Schlessinger AR, Cowan WM, Gottlieb DI. An autoradiographic study of the time of origin and the pattern of granule cell migration in the dentate gyrus of the rat. J Comp Neurol. 1975; 159:149–175. [PubMed: 1112911]

Schobitz B, Voorhuis DA, De Kloet ER. Localization of interleukin 6 mRNA and interleukin 6 receptor mRNA in rat brain. Neurosci Lett. 1992; 136:189–192. [PubMed: 1641189]

Seaberg RM, van der Kooy D. Adult rodent neurogenic regions: the ventricular subependyma contains neural stem cells, but the dentate gyrus contains restricted progenitors. J Neurosci. 2002; 22:1784–1793. [PubMed: 11880507]

Shetty AK, Hattiangady B, Rao MS, Shuai B. Deafferentation enhances neurogenesis in the young and middle aged hippocampus but not in the aged hippocampus. Hippocampus. 2010

Shu HF, Zhang CQ, Yin Q, An N, Liu SY, Yang H. Expression of the interleukin 6 system in cortical lesions from patients with tuberous sclerosis complex and focal cortical dysplasia type IIb. J Neuropathol Exp Neurol. 2010; 69:838–849. [PubMed: 20613633]

Sparkman NL, Johnson RW. Neuroinflammation associated with aging sensitizes the brain to the effects of infection or stress. Neuroimmunomodulation. 2008; 15:323–330. [PubMed: 19047808]

Spulber S, Oprica M, Bartfai T, Winblad B, Schultzberg M. Blunted neurogenesis and gliosis due to transgenic overexpression of human soluble IL-1ra in the mouse. Eur J Neurosci. 2008; 27:549–558. [PubMed: 18279308]

Streit WJ. Microglial senescence: does the brain's immune system have an expiration date? Trends Neurosci. 2006; 29:506–510. [PubMed: 16859761]

Taga T, Fukuda S. Role of IL-6 in the neural stem cell differentiation. Clin Rev Allergy Immunol. 2005; 28:249–256. [PubMed: 16129909]

Taupin P. Adult neurogenesis, neuroinflammation and therapeutic potential of adult neural stem cells. Int J Med Sci. 2008; 5:127–132. [PubMed: 18566676]

Tsakiri N, Kimber I, Rothwell NJ, Pinteaux E. Interleukin-1-induced interleukin-6 synthesis is mediated by the neutral sphingomyelinase/Src kinase pathway in neurones. Br J Pharmacol. 2008a; 153:775–783. [PubMed: 18059318]

Tsakiri N, Kimber I, Rothwell NJ, Pinteaux E. Mechanisms of interleukin-6 synthesis and release induced by interleukin-1 and cell depolarisation in neurones. Mol Cell Neurosci. 2008b; 37:110–118. [PubMed: 17933551]

Vallieres L, Campbell IL, Gage FH, Sawchenko PE. Reduced hippocampal neurogenesis in adult transgenic mice with chronic astrocytic production of interleukin-6. J Neurosci. 2002; 22:486–492. [PubMed: 11784794]

Walker TL, White A, Black DM, Wallace RH, Sah P, Bartlett PF. Latent stem and progenitor cells in the hippocampus are activated by neural excitation. J Neurosci. 2008; 28:5240–5247. [PubMed: 18480280]

Wang K, Yuan CP, Wang W, Yang ZQ, Cui W, Mu LZ, Yue ZP, Yin XL, Hu ZM, Liu JX. Expression of interleukin 6 in brain and colon of rats with TNBS-induced colitis. World J Gastroenterol. 2010; 16:2252–2259. [PubMed: 20458762]

Wang X, Fu S, Wang Y, Yu P, Hu J, Gu W, Xu XM, Lu P. Interleukin-1beta mediates proliferation and differentiation of multipotent neural precursor cells through the activation of SAPK/JNK pathway. Mol Cell Neurosci. 2007; 36:343–354. [PubMed: 17822921]

Weng L, Dai H, Zhan Y, He Y, Stepaniants SB, Bassett DE. Rosetta error model for gene expression analysis. Bioinformatics. 2006; 22:1111–1121. [PubMed: 16522673]

Wesche H, Korherr C, Kracht M, Falk W, Resch K, Martin MU. The interleukin-1 receptor accessory protein (IL-1RAcP) is essential for IL-1-induced activation of interleukin-1 receptor-associated kinase (IRAK) and stress-activated protein kinases (SAP kinases). J Biol Chem. 1997; 272:7727–7731. [PubMed: 9065432]

Ye SM, Johnson RW. Increased interleukin-6 expression by microglia from brain of aged mice. J Neuroimmunol. 1999; 93:139–148. [PubMed: 10378877]

Ye SM, Johnson RW. Regulation of interleukin-6 gene expression in brain of aged mice by nuclear factor kappaB. J Neuroimmunol. 2001; 117:87–96. [PubMed: 11431008]

Yokoyama A, Yang L, Itoh S, Mori K, Tanaka J. Microglia, a potential source of neurons, astrocytes, and oligodendrocytes. Glia. 2004; 45:96–104. [PubMed: 14648550]

Yoshimizu T, Chaki S. Increased cell proliferation in the adult mouse hippocampus following chronic administration of group II metabotropic glutamate receptor antagonist, MGS0039. Biochem Biophys Res Commun. 2004; 315:493–496. [PubMed: 14766235]
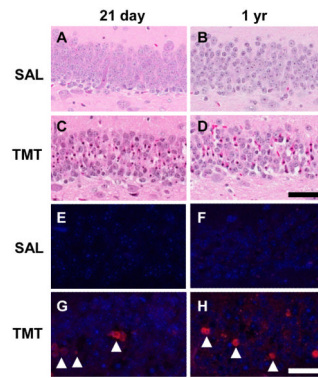
Figure 1.
(A-D) Representative hematoxylin and eosin (H&E) staining in the subgranular zone (SGZ) and granule cell layer (GCL) of the dentate gyrus (DG) in CD-1 male mice. Twenty one day-old (A) and 1 yr-old (B) saline control, or 21 day-old (C) and 1 yr-old (B) at 48 h post-TMT (2.3 mg/kg i.p.). (C & D) Eosin+ staining (deep pink) of neurons displaying nuclear pyknosis and karyolysis indicated an equivalent level of neuronal death (represented by a severity score of 3-4 as defined in Methods). (E-H) Representative immunofluorescent staining for fractin (red; arrowheads) and DAPI (blue) in the GCL. Scale bar = 50 μm.
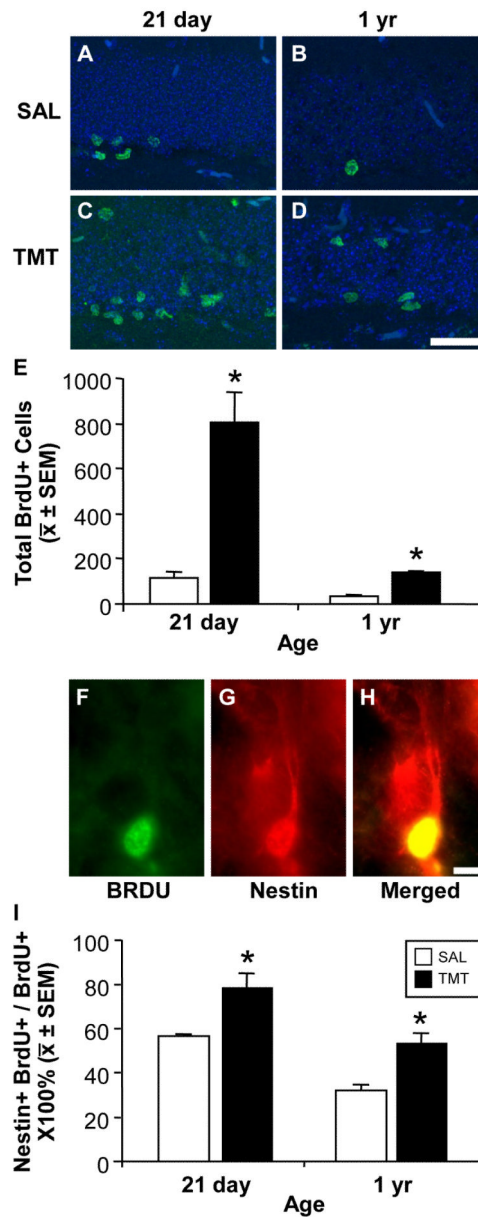
Figure 2.
(A-D) Representative immunofluorescent images of 5′-bromo-2′-deoxyuridine (BrdU) (green) and DAPI (blue) in the SGZ and GCL (A, B) along the inner cell layer of saline control mice and (C, D) within the GCL 48 h post- TMT (2.3 mg/kg i.p.). Scale bar = 50 μm. (E) Unbiased stereology of the number of BrdU+ determined by rare events protocol as described in Methods. Data represents mean ± SEM as defined in Methods and analyzed by a 2×2 ANOVA followed Bonferonni post hoc test (*$p < 0.05$). (F-H) Representative immunostaining of BrdU+ cells co-localized with nestin at 48 h post-TMT. Scale bar = 10 μm (I) Mean + SEM number of BrdU+ cells that co-stained with nestin within the SGZ and GCL. Data analyzed by a 2×2 ANOVA followed by Bonferonni post hoc test (*$p < 0.05$).
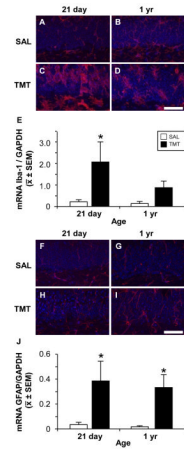
Figure 3.
Representative images of Iba-1+ microglia (A-D, red) and GFAP+ astrocytes (F-I, red), DAPI (A-D, F-I, blue), in the GCL and SGZ (lower portion of each image) in saline control and 48 h post-TMT CD-1 male 21 day-old or 1 yr-old mice. (A) Iba-1+ cells in control 21 day-old mice showed thin elongated processes with distal ramifications. (B) Iba-1+ cells (red) in 1 yr-old mice showed increased staining thickened processes with proximal arborization. With TMT (C) Iba-1+ cells differentiated to a rounded amoeboid morphology in the GCL and cells with enlarged cell bodies and retracted processes in the hilus in the 21 day-old and (D) process bearing cells showing thickened and retracted processes in the 1 yr-old. (F-I) GFAP+ astrocytes (red) showing thin processes through the GCL in (F, G) control and an increased staining at 48 h post-TMT in both (H) 21 day-old and 1 yr-old (I). Scale bar = 50 μm. (E, J) qRT-PCR mRNA levels for Iba-1 and GFAP relative to GAPDH. (E) mRNA levels for Iba-1 were significantly elevated in the 21 day-old at 48 h post-TMT. (J) mRNA levels for GFAP were significantly elevated in the 21 day-old and 1 yr-old mice 48 h post-TMT. Data represents mean ± SEM. Data analyzed by a 2×2 ANOVA followed by Bonferonni post hoc test (*$p<0.05$).
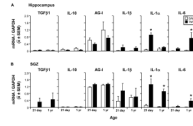
Figure 4.
qRT-PCR mRNA levels of TGFβ1, IL-10, AG-I, IL-1β, IL-α, and IL-6 in the (A)
hippocampus and (B) laser-capture microdissected subgranular zone (SGZ) of 21 day-old
and 1 yr-old saline and TMT treated mice at 48 h post-TMT (2.3 mg/kg, i.p.). Data
represents mean ± SEM mRNA expression relative to GAPDH (n=6) analyzed by a 2×2
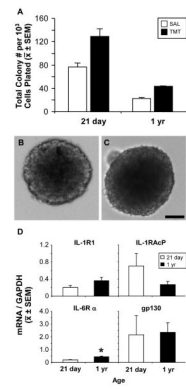ANOVA followed by Bonferonni post hoc test (*p<0.05).

Figure 5.
(A) Proliferation of neurospheres as indicated by determining the mean total numbers of colonies formed per 10^3 cells plated from the hippocampus of 21 day-old and 1 yr-old mice 48 h post-TMT (2.3 mg/kg, i.p.) or saline. Data represents mean ± SD (n=2). (B-C) Representative images of neurospheres obtained from the hippocampus of (B) 21 day-old or (C) 1 yr-old mice. Scale bar = 100 μm.
(D) qRT-PCR for mRNA levels of IL-1R1, IL-RAcP, IL-6Rα, and gp130 within neurospheres isolated from the hippocampus of 21 day or 1 yr-old mice. Data represents mean ± SEM transcript level relative to GAPDH (*p<0.05).
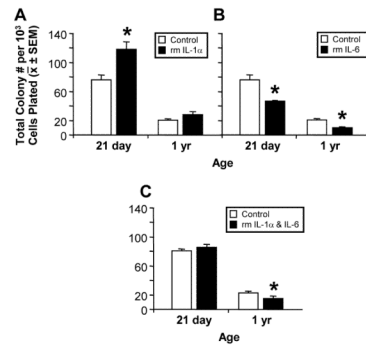
Figure 6.
Differential effects of 21 day exposure to recombinant mouse (A) IL-1α [150 pg/ml], (B) IL-6 [10 ng/ml], or (C) IL-1α [150 pg/ml] and IL-6 [10 ng/ml] protein on neural colony formation. Data represents the mean total colony number per 10^3 cells plated ± SEM. Data (A,B) was analyzed by a 2×2 ANOVA followed by Bonferonni post hoc test or (C) Student t-test (*$p < 0.05$).
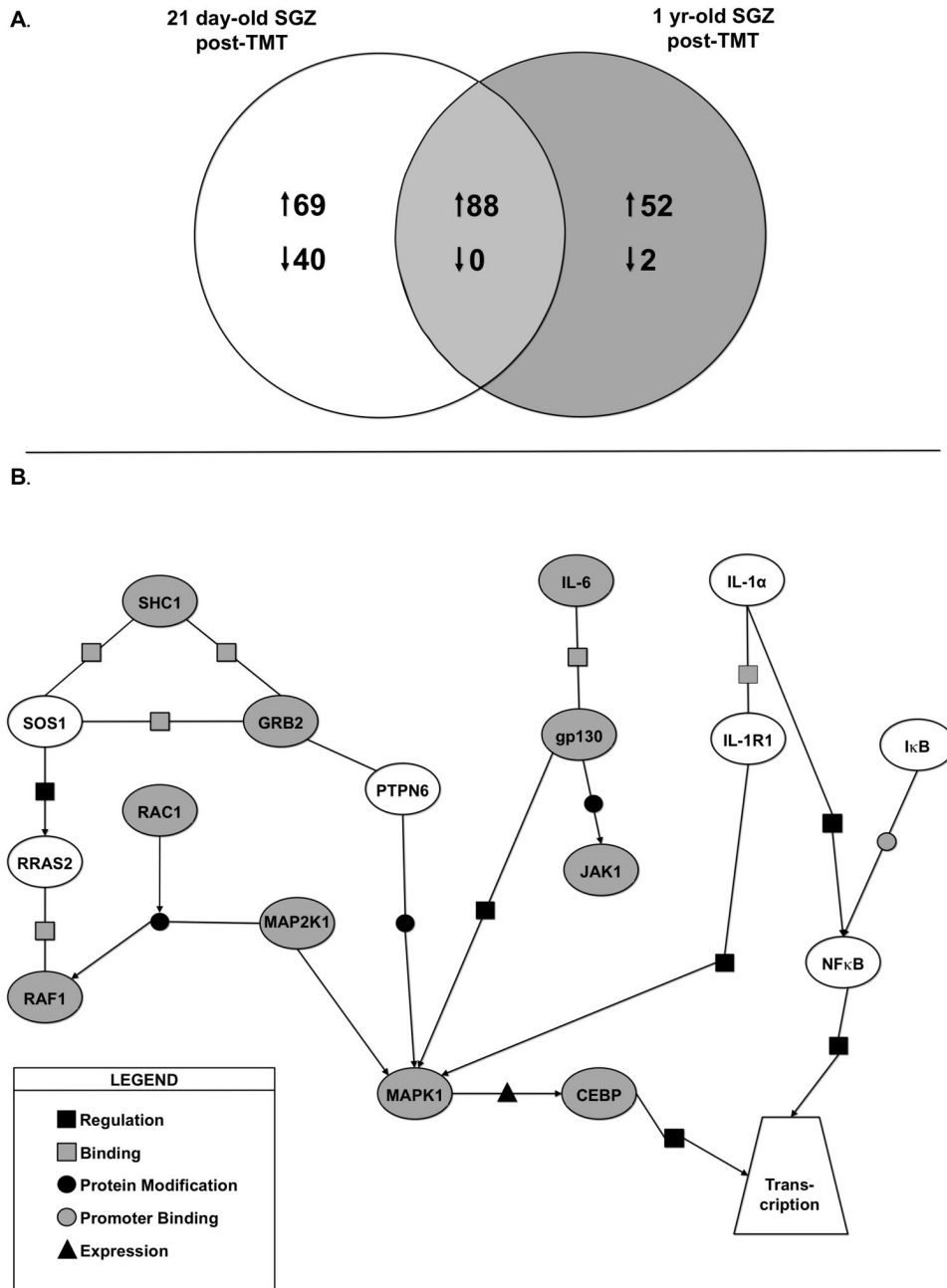
A.

21 day-old SGZ
post-TMT

1 yr-old SGZ
post-TMT

↑69 ↑88 ↑52
↓40 ↓0 ↓2

B.

LEGEND

■ Regulation
▪ Binding
● Protein Modification
● Promoter Binding
▲ Expression

Figure 7.
ANOVA was used to identify genes differentially expressed in TMT-treated versus saline-treated SGZs while taking into account the age-related interaction. (A) Venn diagram represents differentially expressed genes (1.2-fold or greater) by two-way error weighted ANOVA (ANOVA $p<0.001$ with Benjamini-Hochberg FDR $p<0.05$). (B) Graphical representation of differentially expressed genes following TMT-induced injury in 21 day-old versus 1 yr-old mice created using Pathway Archictect. Genes were then further analyzed using the categories of binding, expression, metabolism, promoter binding, protein modification and regulation (see legend). In this analysis, age was considered a mediator of injury related differential expression patterns using ANOVA. These data suggest key

molecules in the IL-6 signaling pathway are upregulated (grey ovals) in the 1 yr-old SGZ following injury. Alternatively, IL-1α pathway genes are upregulated (white ovals) in the young SGZ following injury.